PNAS

Supporting Information for

Basis for high-affinity ethylene binding by the ethylene receptor ETR1 of Arabidopsis

Beenish J. Azhar[1,2], Safdar Abbas[1,2], Sitwat Aman[1], Maria V. Yamburenko[1], Wei Chen[1], Lena Müller[3], Buket Uzun[3], David A. Jewell[1], Jian Dong[1], Samina N. Shakeel[1,2], Georg Groth[3], Brad M. Binder[4], Gevorg Grigoryan[1,5]*, G. Eric Schaller[1]*

G. Eric Schaller, Gevorg Grigoryan
Email: george.e.schaller@dartmouth.edu; gevorg.grigoryan@dartmouth.edu

This PDF file includes:

Supplemental Materials and Methods
Figures S1 to S9
Tables S1 to S2

Other supporting materials for this manuscript include the following:

Movies S1 to S2.

Materials and Methods

Plant materials and growth conditions

All Arabidopsis lines were of the Columbia (Col-0) accession. The *etr1-1* and *etr1-6 etr2-3 ein4-4* mutant lines have been described (1-3). Analysis of the triple response of dark-grown Arabidopsis seedlings to ethylene was performed as described (4). Briefly, seedlings were grown at 22˚C on vertically oriented plates on half-strength Murashige and Skoog basal medium with Gamborg's vitamins (pH 5.75; Sigma), 0.8% (w/v) agar, and 5 μM aminoethoxyvinylglycine (AVG) to inhibit ethylene biosynthesis. The stratified seed was exposed to light for 8 hr then moved to the dark in the presence or absence of ethylene, with analysis of the seedling growth being performed following 4 days total growth. Inhibition of seedling ethylene responses was accomplished by growth with 100 μM silver nitrate or treatment with 1 μL L^{-1} 1-methylcyclopropene (1-MCP) (5). For short-term kinetic analysis of dark-grown seedlings, time-lapse imaging and growth rate analysis of hypocotyls were carried out as described (6, 7).

Generation of site-directed mutations

ETR1 constructs used for expression in Arabidopsis were all derived from a 7.3-kb genomic ETR1 fragment containing the full-length coding sequence and native genomic promoter in the vector pCAMBIA1380 (8). Site directed mutagenesis was performed according to the manufacturers with the QuikChangeII XL Site Directed Mutagenesis Kit (Agilent Technologies) for mutations of Asp25 or with the Q5 Site-Directed Mutagenesis kit (NEB) for mutations at other sites. Primers used for mutagenesis are listed in Table S2. For plant transformation, constructs were introduced into *Agrobacterium tumefaciens* strain GV3101 and transformed into the *etr1-6 etr2-3 ein4-4* background (3) by the floral-dip method (9). Lines containing single sites of insertion for the transgene were identified based on segregation of hygromycin resistance and brought to homozygosity for analysis.

ETR1 constructs used for expression in yeast were all derived from an ETR1 cDNA driven by the ADH1 promoter in the vector pYcDE-2 (10). Site-directed mutations of Asp25 were introduced using the same primers and methodologies described above for expression of ETR1 in Arabidopsis. Mutations of Lys91 were introduced by replacing a Msc I-Sac I restriction fragment in the ETR1 cDNA with that from the genomic ETR1 mutant. Yeast constructs were transformed into the yeast *Saccharomyces cerevisiae* strain FY834 (MATα his3Δ200 ura3-52 leu2Δ1 lys2Δ202 trp1Δ63 GAL2+) (11).

Generation of CRISPR-Cas9 mutant lines targeting *ERS1* and *ERS2*

To target *ERS1* and *ERS2*, a tandem CRISPR cassette was synthesized that encoded four sgRNAs (two against *ERS1* and two against *ERS2*) driven by U6 promoters and surrounded by Hpa I and Nae I sites and cloned into pUC57 (General Biosystems) (Figure S7). The guide RNAs were designed using CRISPR-P 2.0 (12) to introduce indel mutations in the first exons of *ERS1* and *ERS2* that encode the ethylene binding site. The Hpa I/Nae I fragment containing the gRNA cassette was cloned into the Pme I site of the pCAMBIA2300-Cas9 vector, which had been generated by taking the Nsi I/Kpn I restriction fragment with Cas9 from the plasmid pMTN3164 (13) and cloning into the Nsi I/Pst I sites of pCambia2300 GenBank™ accession no. AF234315). The CRISPR-ERS1/ERS2 plasmid was transformed into the Agrobacterium strain GV3101, and the Arabidopsis line $ETR1^{D25N}$-#6 (*etr1 etr2 ein4*) transformed by the floral dip method (9). Heat stress treatment of transgenic lines was used to increase the efficiency of CRISPR-Cas9 mutagenesis (14).

For identification and genotyping of CRISPR/Cas9 mutants, genomic DNA was isolated (15), and the region surrounding the CRISPR target sequence amplified by PCR and sequenced using primers given in Table S2. The presence of the T-DNA insert containing the Cas9 cassette was determined by PCR using primers for the KanR gene (Table S2). Two independent $ETR1^{D25N}$ (*etr1 etr2 ein4 ers1 ers2*) lines were generated (#11 and #15), line #11 being Cas9 (-/-) and line #15 being Cas9(+/+). Characteristics of the indel mutations and lines used for study are given in Figure S7.

Immunoblot analysis

For yeast, total protein was extracted by bead-beating as described (16) using a Mixer Mill 400 tissue homogenizer (Retsch). For plants, microsomes were isolated from seedlings as described (17). ETR1 was identified by use of a polyclonal anti-ETR1 antibody generated against amino acids 401-738 of ETR1 (18). Immunoblot analysis was performed as described (17), using an anti-BIP antibody or Ponceau-S staining for protein as loading controls. Immunodecorated proteins were visualized and quantified by chemiluminescence using the chemiDoc MP imaging system (BIORAD).

Copper binding assay

Copper binding was monitored spectrophotometrically by measuring absorbance of the purple BCA2-Cu(I) complex as described (19). Titration curves were corrected for nonspecific binding observed with chemically and thermally denatured receptor to maximize signal to background levels.

Ethylene binding assay

[^{14}C]ethylene (specific activity = 116 mCi/mmol) was obtained from ViTrax Radiochemicals (Placentia, CA) and trapped as the mercuric perchlorate complex as described (10, 20). For ethylene binding assays in yeast, ETR1 was expressed in the yeast *Saccharomyces cerevisiae* (strain FY834) (11) using the vector pYcDE-2 and a constitutive ADC1 promoter (10, 21). The yeast growth media was supplemented with 40 μg L^{-1} copper sulfate. Saturable ethylene binding to yeast was determined by analyzing binding of 0.3 g yeast per sample to 0.21 μL L^{-1} [^{14}C]ethylene, in the presence or absence of excess [^{12}C]ethylene (10, 20).

For ethylene binding assays with Arabidopsis seedlings, two-week-old green seedlings were used that had been grown on media containing 5 μM AVG to inhibit ethylene biosynthesis, with ~1 g seedlings per sample. The fresh weight of seedlings was determined, and each sample packaged into bags formed from a layer of cheese cloth and stapled at the top. Humidity was maintained in the ethylene binding chambers by use of moistened paper towels. Saturable ethylene binding was determined by analyzing binding to 0.31 μL L^{-1} [^{14}C]ethylene, in the presence or absence of excess [^{12}C]ethylene (10, 20).

RNA Expression Analysis

RNA isolation and RT-qPCR was performed as described (22), with three biological replicates and two technical replicates of each. Primers for genes and the control tubulin gene used for normalization are listed in Table S2.

Evolutionary analysis to predict contacting residues of ETR1

For the coevolutionary analysis we used EVCOUPLINGS and GREMLIN web servers to predict interactions/contacting residues in the EBD of ETR1 (23, 24). The 1-112 amino-acid sequence of ETR1 was used as an input for both servers. The EVCOUPLINGs algorithm derives residue-residue evolutionary couplings (ECs) from deep multiple sequence alignment by pseudo-likelihood maximization method. We used the default settings for finding the evolutionary couplings between contacting residues where residue contact distance threshold was set to 5 and maximum rank was 1. Results are reported for the recommended result, which is based on the analysis of 1221 sequences and an overall quality score of 9 (Table S1). For GREMLIN, the multiple sequence alignment was performed by HHBLITS and the alignment then filtered to remove regions where the gap was greater than 75.

Structural models of the EBD

An *ab initio* structural model of the EBD has been previously described (19). New structural models for the ETR1 homodimer were generated for full-length ETR1 as well as for the EBD (amino acids 1-128) with AlphaFold-Multimer, which builds on the neural network-based AlphaFold to generate structural models of protein complexes (25, 26). Coppers were modeled under two potential coordinations involving Cys65 and His69 of the ETR1 homodimer, one in which the two coppers are bound independently and do not share an interaction with each other, and another where they are closely bonded. Molecular graphics were generated with the PyMOL Molecular Graphics System, Version 2.5 Schrödinger, LLC and with USCF ChimeraX, Version

1.4 (27). Coordinates of the full-length ETR1 structural models with copper are available as PDB and PyMOL files at https://digitalcommons.dartmouth.edu/facoa/4313.

Statistical Analysis
Unpaired T-tests were performed in Prism (GraphPad Software, Inc.), without the assumption of a consistent SD, to obtain the individual P values. ANOVA-based statistical analyses were performed using an online calculator (astatsa.com/OneWay_Anova_with_TukeyHSD/).

Gene Identifiers
ETR1 (At1g66340), *ETR2* (At3g23150), *EIN4* (At3g04580), *ERS1* (At2g40940), *ERS2* (At1g04310), *ERF1* (At3g23240), *ARGOS* (At3g59900), *OSR1* (At2g41230), *EXP5* (At3g29030), *EXPb1* (At2g20750), *CAPE2* (At4G25780), *B-TUB3* (At5G62700)

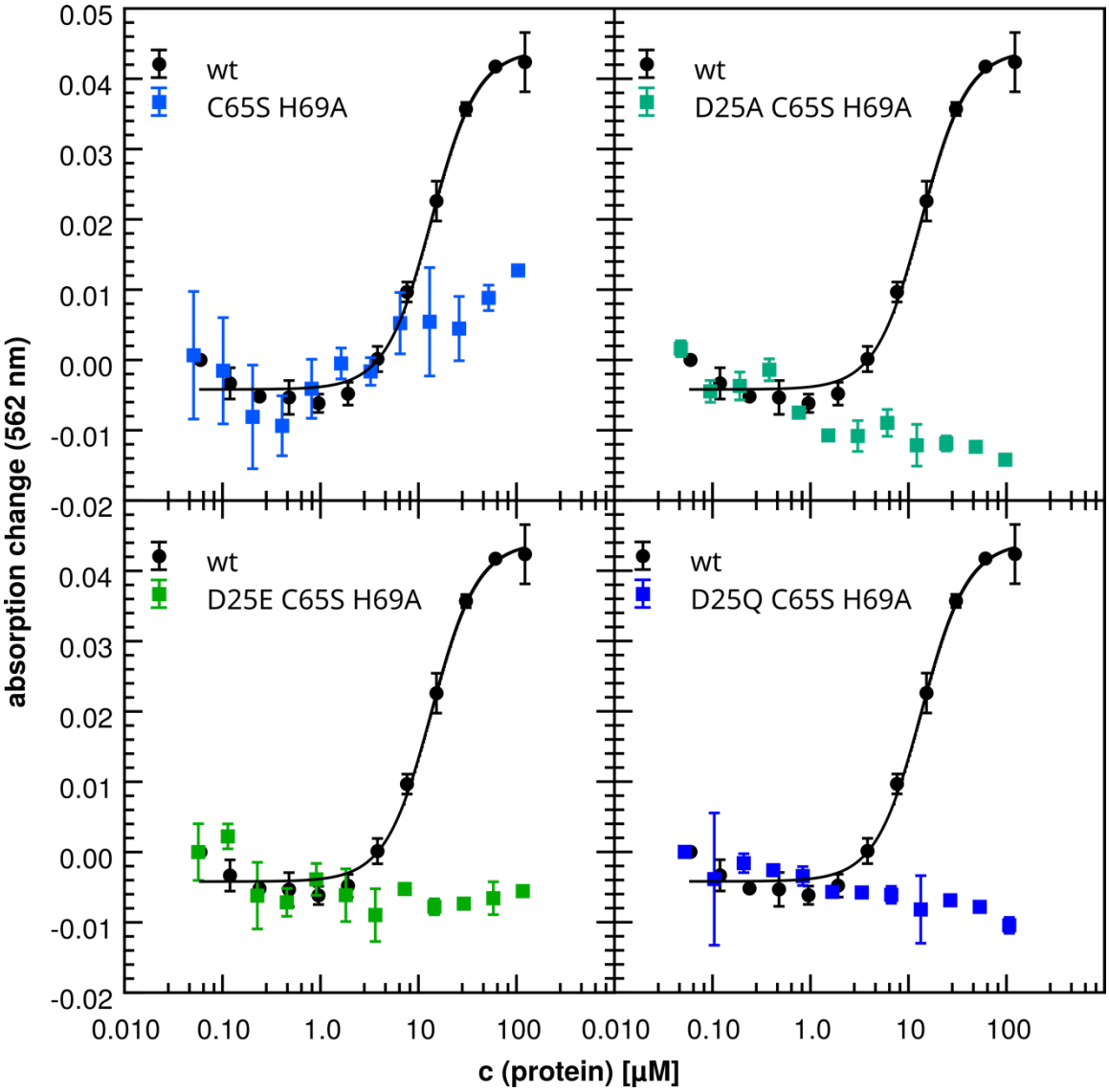

Figure S1. Copper binding by wild-type, Cys65 His69 double mutant, and Asp25 mutant versions of ETR1

Copper binding of wild-type and mutant versions of ETR1 transmembrane domain (ETR1-TMD; n = 3). Purified ETR1-TMD was titrated to the BCA_2-Cu(I) complex, and copper binding monitored spectrophotometrically based on the change in absorbance at 562 nm. For comparison, copper binding of a Cys65Ser His69Ala mutation was examined alone and in combination with the Asp25 mutations.

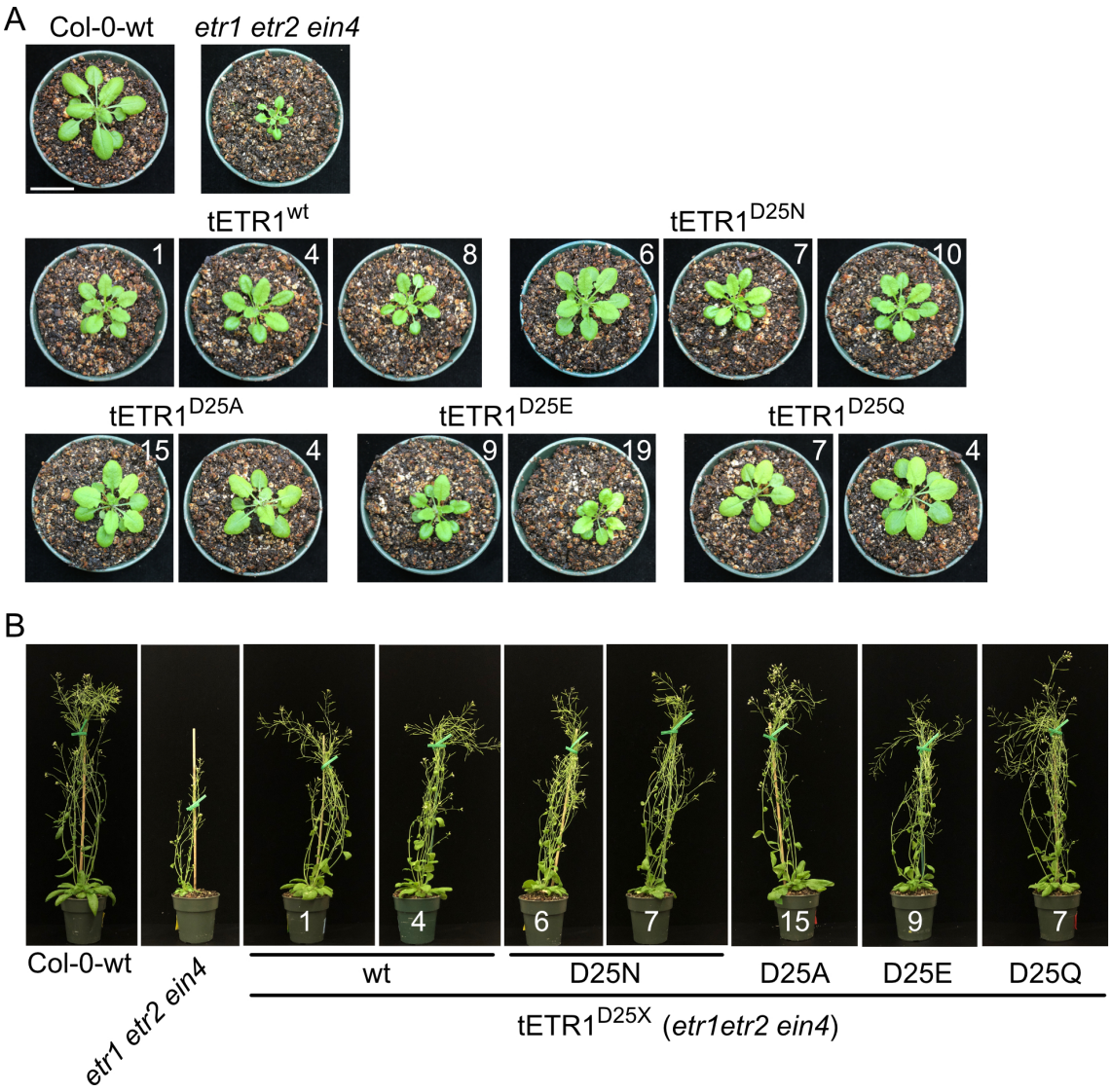

Figure S2. Adult plant phenotypes of ETR1^{D25X} mutants
The tETR1^{D25X} plants in the *etr1 etr2 ein4* background are compared to the wild type and the *etr1 etr2 ein4* mutant. The *etr1 etr2 ein4* mutant exhibits reduced growth due to its partial constitutive ethylene-response phenotype, and this can be rescued by transgenic expression of *ETR1*. The tETR1^{D25X} line numbers are indicated.
(A) Representative rosettes of 28-day-old plants. Scale bar = 2 cm.
(B) Representative adult plants with inflorescences.

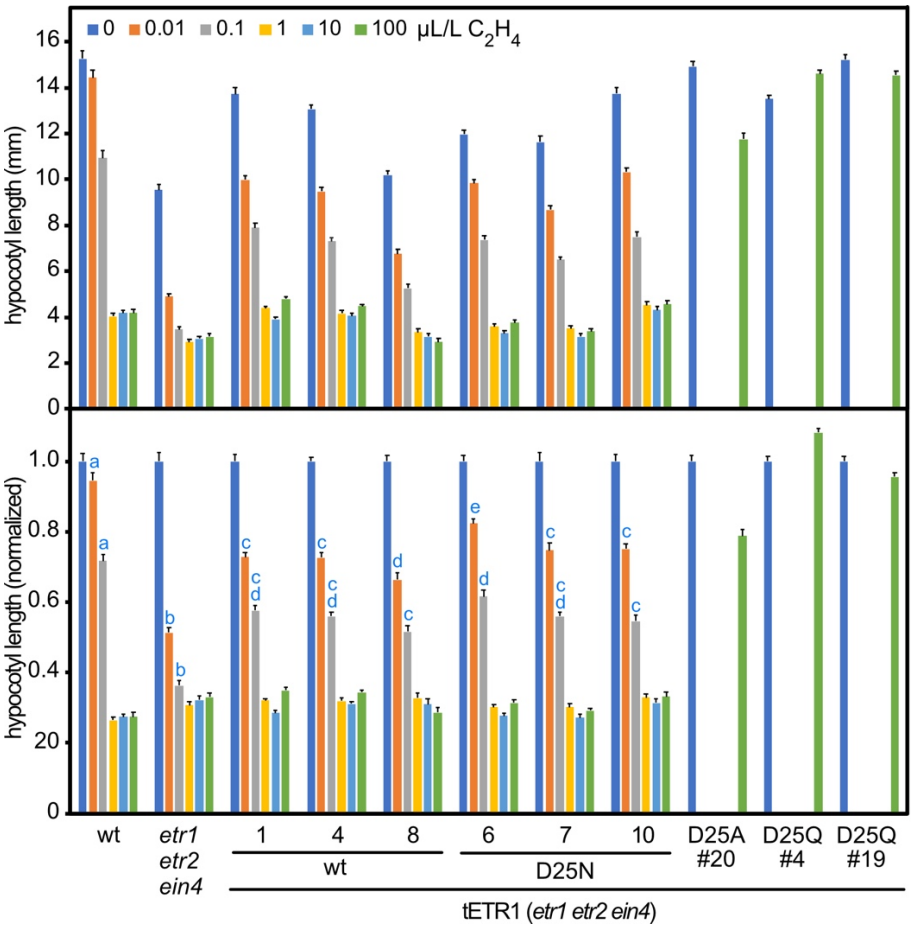

Figure S3. Ethylene dose response analysis of Arabidopsis seedlings expressing Asp25 mutants (bar graphs of data from Figure 2C). Hypocotyl growth in dark-grown seedlings for the wild type (wt), the *etr1 etr2 ein4* triple mutant, and the triple mutant complemented with $ETR1^{wt}$ or $ETR1^{D25}$ was determined at 0, 0.01. 0.1, 1, 10, and 100 µL/L ethylene. Representative ethylene-insensitive $tETR1^{D25A}$-#20, $tETR1^{D25E}$-#19, and $tETR1^{D25Q}$-#4 lines were also included and examined at 0 and 100 µL L^{-1} ethylene. The growth response is graphed based on hypocotyl length in mm (top) and normalized for each line relative to its hypocotyl length at 0 µL/L ethylene (bottom) (n ≥ 17; error bar = SE). For the normalized hypocotyl length, different blue letters indicate a significant difference between lines at 0.01 and 0.1 µL/L ethylene (ANOVA with post-hoc Holm multiple comparison calculation; $P<0.05$).

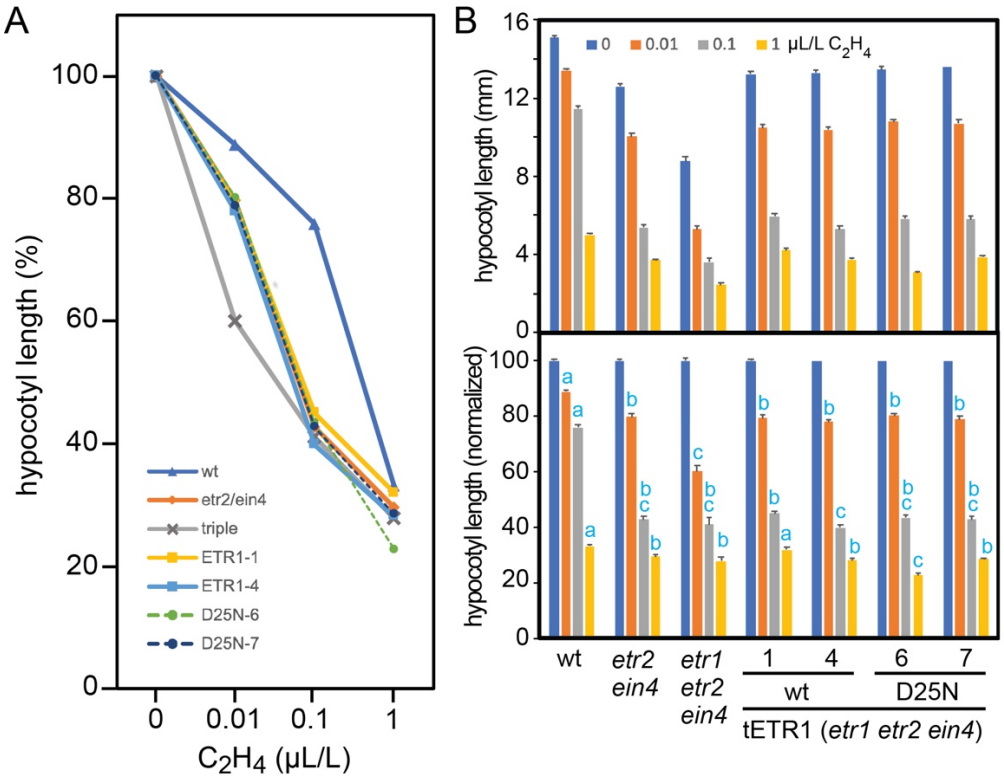

Figure S4. The ETR1^{wt} or ETR1^{D25N} transgenic lines in the *etr1 etr2 ein4* background exhibit similar ethylene sensitivity to an *etr2 ein4* mutant. Hypocotyl growth in dark-grown seedlings for the wild type (wt), the *etr2 ein4* double mutant, the *etr1 etr2 ein4* triple mutant, and two lines each for the triple mutant complemented with ETR1^{wt} or ETR1^{D25N} was determined at 0, 0.01. 0.1, and 1 µL/L ethylene (n ≥ 10). (A) Dose response curves. The ethylene response is normalized for each line relative to its hypocotyl length at 0 µL/L ethylene (SE not shown for clarity). (B) Bar graphs of data. The growth response is graphed based on hypocotyl length in mm (top) and normalized for each line relative to its hypocotyl length at 0 µL/L ethylene (bottom) (error bar = SE). For the normalized hypocotyl length, different blue letters indicate a significant difference between lines at 0.01, 0.1, and 1 µL/L ethylene (ANOVA with post-hoc Holm multiple comparison calculation; $P<0.05$).

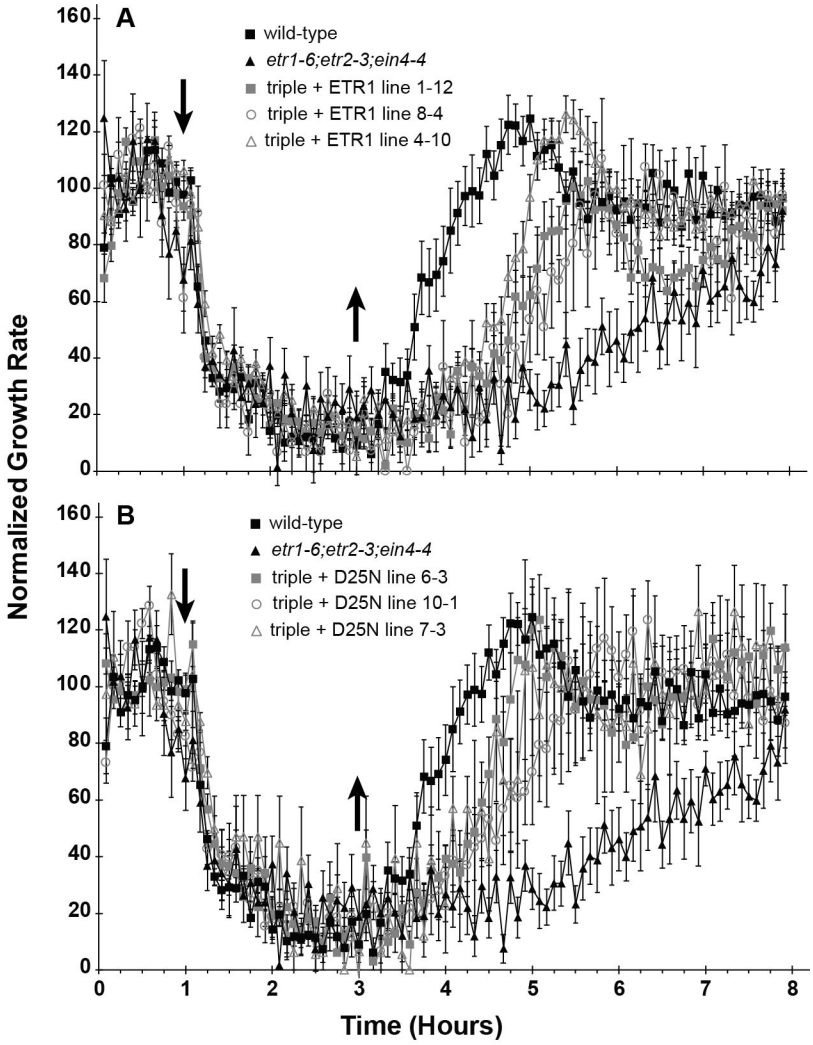

Figure S5. Kinetics of growth response to ethylene of ETR1^{wt} and ETR1^{D25N} lines
Ethylene dose response kinetics were analyzed in hypocotyls of 2-d-old etiolated seedlings for wild type, the *etr1 etr2 ein4* triple mutant, and for the triple mutant complemented with ETR1^{wt} (panel A) or ETR1^{D25N} (panel B). Measurements were made in air for 1 hr, followed by a 2-hr exposure to 10 μL L^{-1} ethylene, and then a 5-hr recovery in air. Growth rates for each line are normalized to the growth rate during the first hour in the air. Arrows indicate the time points for the addition and removal of ethylene. Error bars represent SE (n≥9 for all lines, except for ETR1 line 8, n=4).

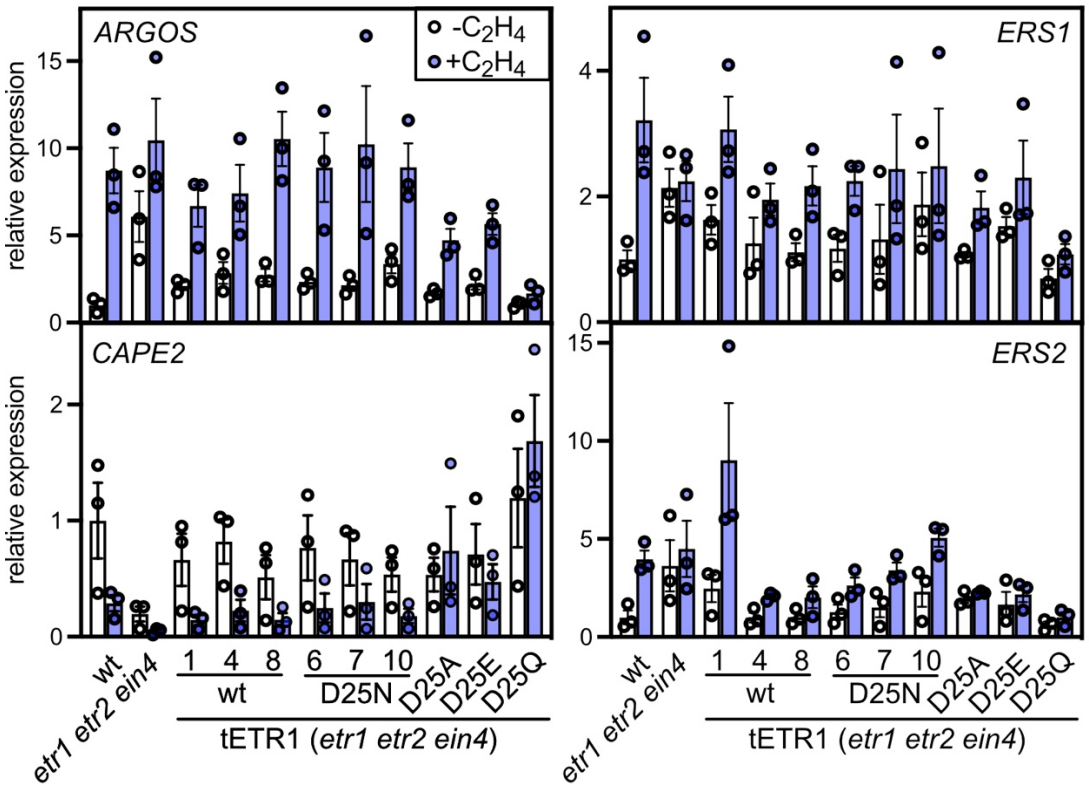

Figure S6. Effect of ETR1 Asp25 mutants on ethylene-dependent gene expression. Dark-grown seedlings were treated with 0 or 1 μL L^{-1} ethylene for 2 hr, and gene expression examined by RT-qPCR (n=3). Expression was normalized to a tubulin control and is presented as relative to the untreated wild-type control. Three tETR1-wt and three $tETR1^{D25N}$ lines were examined. The ethylene-insensitive $tETR1^{D25A}$#20, $tETR1^{D25E}$#19, and $tETR1^{D25Q}$#4 lines were also included.

A

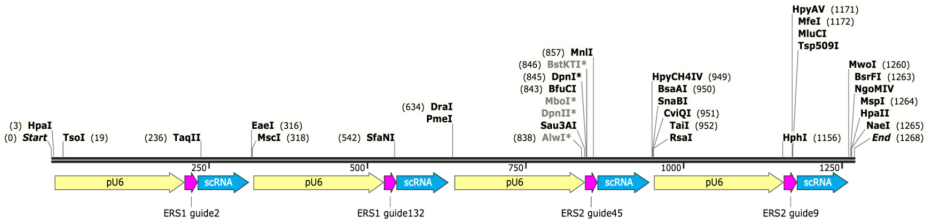


```
gttaacCATCTTCATTCTTAAGATATGAAGATAATCTTCAAAAGGCCCCTGGGAATCTGAAAGAAGAGAAGCAGGCCCATTTATATGGGAAAGAACAATAGTATTTCTTA  110
TATAGGCCCATTTAAGTTGAAAACAATCTTCAAAAGTCCCACATCGCTTAGATAAGAAAACGAAGCTGAGTTTATATACAGCTAGAGTCGAAGTAGTGATTGgcataagc  220
acccatttgtaaGTTTTAGAGCTAGAAATAGCAAGTTAAAATAAGGCTAGTCCGTTATCAACTTGAAAAAGTGGCACCGAGTCGGTGCTTTTTTTTGGCCACATCTTCAT  330
TCTTAAGATATGAAGATAATCTTCAAAAGGCCCCTGGGAATCTGAAAGAAGAGAAGCAGGCCCATTTATATGGGAAAGAACAATAGTATTTCTTATATAGGCCCATTTAA  440
GTTGAAAACAATCTTCAAAAGTCCCACATCGCTTAGATAAGAAAACGAAGCTGAGTTTATATACAGCTAGAGTCGAAGTAGTGATTGtcaacgcatctgagatgtatGTT  550
TTAGAGCTAGAAATAGCAAGTTAAAATAAGGCTAGTCCGTTATCAACTTGAAAAAGTGGCACCGAGTCGGTGCTTTTTTTGTTTAAACCATCTTCATTCTTAAGATATGA  660
AGATAATCTTCAAAAGGCCCCTGGGAATCTGAAAGAAGAGAAGCAGGCCCATTTATATGGGAAAGAACAATAGTATTTCTTATATAGGCCCATTTAAGTTGAAAACAATC  770
TTCAAAAGTCCCACATCGCTTAGATAAGAAAACGAAGCTGAGTTTATATACAGCTAGAGTCGAAGTAGTGATTGatcctcaactcgcaaaaagtGTTTTAGAGCTAGAAA  880
TAGCAAGTTAAAATAAGGCTAGTCCGTTATCAACTTGAAAAAGTGGCACCGAGTCGGTGCTTTTTTTTACGTACATCTTCATTCTTAAGATATGAAGATAATCTTCAAAA  990
GGCCCCTGGGAATCTGAAAGAAGAGAAGCAGGCCCATTTATATGGGAAAGAACAATAGTATTTCTTATATAGGCCCATTTAAGTTGAAAACAATCTTCAAAAGTCCCACA  1100
TCGCTTAGATAAGAAAACGAAGCTGAGTTTATATACAGCTAGAGTCGAAGTAGTGATTGgccttcaccttacaattgggGTTTTAGAGCTAGAAATAGCAAGTTAAAATA  1210
AGGCTAGTCCGTTATCAACTTGAAAAAGTGGCACCGAGTCGGTGCTTTTTTTGCCGGC  1268
```

B

ERS1 (wt)

TTAGTGAAGTACCAATACATCTCAGATGCGTTGATTGCTCTTGCATACTTCTCAATCCCACTCGAGCTTATCTATTTCGTGCAAA
guide 132
AGTCTGCTTTCTTCCCTTACAAATGGGTGCTTATGCAGTTTGGA
guide 2

ERS1 (ETR1^{D25N} #11)

TTAGTGAAGTACCAATATCATCTCAGATGCGTTGATTGCTCTTGCATACTTCTCAATCCCACTCGAGCTTATCTATTTCGTGCAA
AAGTCTGCTTTCTTCCCTTACAAATGGGTGCTTATGCAGTTTGG

ERS1 (ETR1^{D25N} #15)

TTAGTGAAGTACCAATAC**(atctcagatgcgttgattgctcttgcatacttctcaatcccactcgagcttatctatttcgtgcaaaagtctgctttcttcccttac)**AAAT
GGGTGCTTATGCAGTTTGG

ERS2 (wt)

TACGAGACAATCCTCAACTCGCAAAAAGTCGGCGACTTTCTTATCGCAATCGCTTATTTCTCGATCCCAATCGAGCTGGTTTAC
guide 45
TTCGTGAGCCGCACCAATGTGCCTTCACCTTACAATTGGGTGGTCTGCGAGTTT
guide 9

ERS2 (ETR1^{D25N} #11)

TACGAGACAATCCTCAACTCGCAAAAAGTCGGCGACTTTCTTATCGCAATCGCTTATTTCTCGATCCCAATCGAGCTGGTTTAC
TTCGTGAGCCGCACCAATGTGCCTTCACCTTACAAT**(t)**GGGTGGTCTGCGAGTTT

ERS2 (ETR1^{D25N} #15)

TACGAGACAATCCTCAACTCGCAAAA**(a)GACGAC**GTCGGCGACTTTCTTATCGCAATCGCTTATTTCTCGATCCCAATCGAGC
TGGTTTACTTCGTGAGCCGCACCAATGTGCCTTCACCTTACA**(att)**GGGTGGTCTGCGAGTTT

Figure S7. CRISPR-Cas9 targeting of *ERS1* and *ERS2*
(A) Diagram and sequence for CRISPR-Cas9 cassette targeting *ERS1* and *ERS2*.
(B) CRISPR-Cas9 induced mutations in *ERS1* and *ERS2*. Nucleotide sequences are given for the wild-type *ERS1* and *ERS2* sequences as well as for the *ERS1* and *ERS2* sequences found for the *ETR1^{D25N} #11* and *#15* lines in the *etr1 etr2 ers1 ers2 ein4* background. Positions of the guide RNAs are indicated for the wild-type sequences. Gray highlights indicate sequence encoding TM1 and beginning of TM2 in the receptors. Insertion sequences are capitalized, bold, and colored red. Deletion sequences are lower case, bold, colored red, and in parentheses.

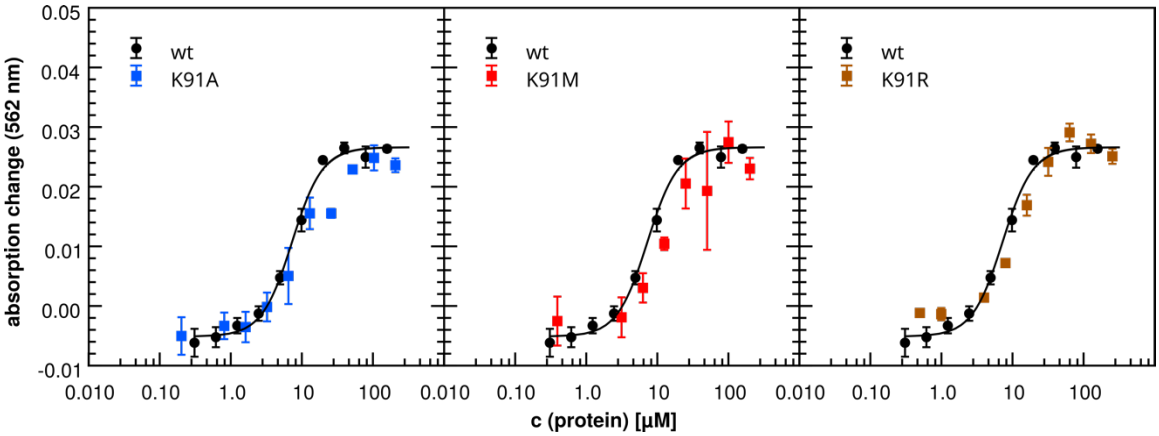

Figure S8. Copper binding by wild-type and Lys91 mutant versions of ETR1
Copper binding of wild-type and Lys91 mutant versions of ETR1 transmembrane domain (ETR1-TMD; n = 3). Purified ETR1-TMD was titrated to the BCA_2-Cu(I) complex, and copper binding monitored spectrophotometrically based on the change in absorbance at 562 nm.

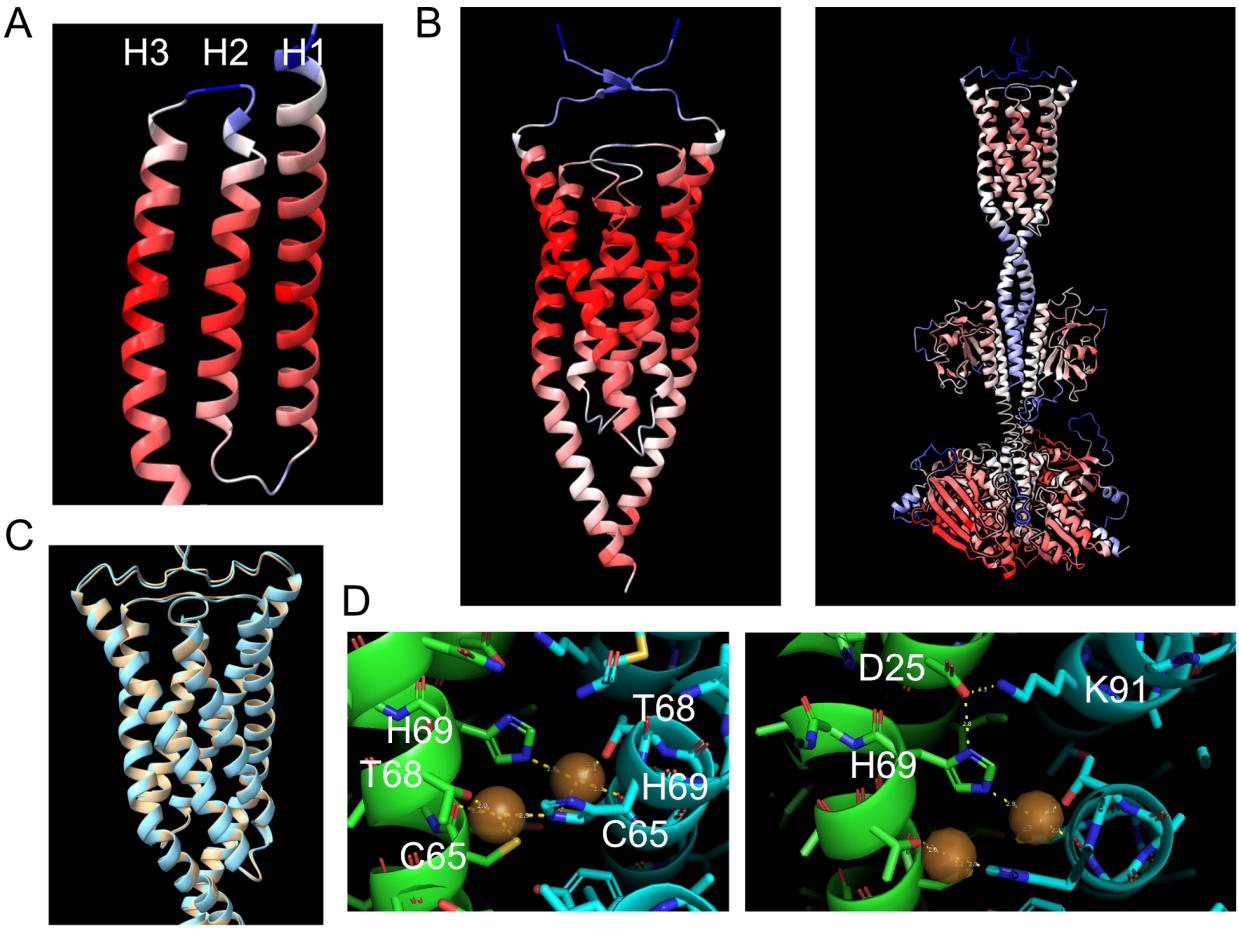

Figure S9. AlphaFold-based models of ETR1
(A) Confidence levels of AlphaFold model for ETR1 transmembrane domain with B-factor range of 56.7 (blue) to 93.7 (red)
(B) AlphaFold-Multimer models with confidence levels for homodimers of the EBD (amino acids 1-128; B factor range 37-97) and full-length ethylene receptor (B factor range 33.1-82).
(C) Overlay of 'relaxed' (cyan) and 'unrelaxed' (tan) multimer models of ETR1 homodimers.
(D) AlphaFold-Multimer-based model of the ETR1 homodimer (coppers not interacting), with views highlighting copper binding geometry (left; H69-Cu = 2.9 Å, C65-Cu = 2.2 Å, T68-Cu = 2.0 Å, C65backbone carbonyl-Cu = 2.3 Å) and interactions between His69, Asp25, and Lys91 (right; D25-H69 = 2.8 Å, D25-K91 = 3.3 Å).

Table S1. EVcouplings for ETR1 EBD
I and J: residue # of ETR1 amino acid sequence
A_i and A_j: amino acid identity (single letter code)
Seg_i and seg_j: Segments i and j
Prob: probability

I	A_i	j	A_j	cn	seg_i	seg_j	mad_score	prob	score
74	W	80	S	1.17	A	A	19.484	1	12.095
29	A	70	L	1.084	A	A	18.075	1	11.193
33	F	67	A	1.067	A	A	17.795	1	10.947
71	I	90	A	0.831	A	A	13.908	1	8.323
26	F	73	L	0.785	A	A	13.161	1	7.785
20	Y	88	T	0.668	A	A	11.224	0.998	6.482
21	Q	88	T	0.652	A	A	10.96	0.998	6.323
64	L	93	L	0.632	A	A	10.644	0.998	6.081
25	D	91	K	0.609	A	A	10.252	0.997	5.861
27	F	99	C	0.563	A	A	9.51	0.995	5.36
20	Y	92	V	0.559	A	A	9.437	0.995	5.295
60	A	97	V	0.554	A	A	9.347	0.995	5.249
39	L	55	L	0.536	A	A	9.053	0.993	4.957
72	N	91	K	0.533	A	A	9.005	0.992	4.869
38	E	106	V	0.498	A	A	8.427	0.99	4.637
31	A	99	C	0.482	A	A	8.166	0.987	4.312
64	L	97	V	0.46	A	A	7.805	0.985	4.183
22	Y	73	L	0.424	A	A	7.219	0.976	3.716
18	M	76	F	0.386	A	A	6.592	0.965	3.304
38	E	109	I	0.382	A	A	6.521	0.956	3.079
17	L	82	T	0.377	A	A	6.445	0.956	3.07
28	I	68	T	0.362	A	A	6.197	0.955	3.066
24	S	92	V	0.355	A	A	6.075	0.948	2.907
71	I	83	V	0.341	A	A	5.85	0.946	2.858
43	V	49	F	0.339	A	A	5.809	0.946	2.857
68	T	90	A	0.353	A	A	6.04	0.944	2.83
82	T	89	T	0.331	A	A	5.686	0.944	2.817
72	N	87	M	0.332	A	A	5.708	0.942	2.781
49	F	55	L	0.332	A	A	5.693	0.941	2.772
33	F	66	G	0.338	A	A	5.798	0.934	2.648
43	V	56	V	0.322	A	A	5.544	0.931	2.595
22	Y	76	F	0.314	A	A	5.405	0.925	2.515
40	I	59	G	0.308	A	A	5.306	0.923	2.484
58	F	65	C	0.274	A	A	4.747	0.897	2.166
36	P	62	I	0.277	A	A	4.799	0.892	2.115
41	Y	109	I	0.282	A	A	4.87	0.885	2.038
43	V	55	L	0.261	A	A	4.527	0.881	2
27	F	95	A	0.27	A	A	4.676	0.875	1.943
36	P	101	T	0.251	A	A	4.361	0.871	1.906
32	Y	98	S	0.25	A	A	4.346	0.869	1.895
79	H	87	M	0.261	A	A	4.536	0.868	1.883
45	K	52	R	0.257	A	A	4.464	0.866	1.862
38	E	105	L	0.265	A	A	4.599	0.865	1.858
32	Y	62	I	0.252	A	A	4.387	0.865	1.856
34	S	102	A	0.245	A	A	4.268	0.858	1.796
62	I	69	H	0.236	A	A	4.116	0.848	1.716
11	W	76	F	0.34	A	A	5.826	0.846	1.706
30	I	99	C	0.237	A	A	4.132	0.845	1.693

58	F	69	H	0.23	A	A	4.018	0.84	1.655
28	I	91	K	0.228	A	A	3.986	0.837	1.636
21	Q	91	K	0.24	A	A	4.19	0.836	1.626
35	I	101	T	0.219	A	A	3.842	0.826	1.556
57	Q	97	V	0.225	A	A	3.941	0.824	1.543
61	F	101	T	0.224	A	A	3.927	0.822	1.529
62	I	101	T	0.219	A	A	3.849	0.817	1.497
81	R	98	S	0.221	A	A	3.875	0.812	1.463
61	F	98	S	0.213	A	A	3.743	0.808	1.437
21	Q	87	M	0.216	A	A	3.794	0.801	1.39
34	S	106	V	0.212	A	A	3.73	0.798	1.376
24	S	95	A	0.209	A	A	3.675	0.798	1.375
67	A	90	A	0.207	A	A	3.636	0.795	1.352
54	V	108	I	0.212	A	A	3.719	0.791	1.334
65	C	98	S	0.204	A	A	3.588	0.791	1.332
50	P	59	G	0.196	A	A	3.46	0.78	1.264
61	F	94	T	0.2	A	A	3.524	0.776	1.245
21	Q	72	N	0.205	A	A	3.61	0.775	1.239
28	I	65	C	0.202	A	A	3.56	0.775	1.235
26	F	70	L	0.207	A	A	3.643	0.774	1.231
25	D	101	T	0.189	A	A	3.342	0.769	1.204
32	Y	69	H	0.194	A	A	3.425	0.767	1.193
40	I	56	V	0.191	A	A	3.382	0.765	1.179
25	D	88	T	0.197	A	A	3.472	0.76	1.155
32	Y	65	C	0.189	A	A	3.342	0.759	1.149
27	F	60	A	0.189	A	A	3.341	0.758	1.144
28	I	94	T	0.184	A	A	3.271	0.758	1.14
50	P	106	V	0.194	A	A	3.428	0.753	1.116
30	I	90	A	0.184	A	A	3.267	0.75	1.096
40	I	60	A	0.181	A	A	3.21	0.743	1.059
35	I	61	F	0.178	A	A	3.16	0.735	1.018
52	R	64	L	0.182	A	A	3.24	0.731	1
36	P	66	G	0.178	A	A	3.163	0.727	0.979
25	D	72	N	0.193	A	A	3.412	0.724	0.964
38	E	104	M	0.172	A	A	3.07	0.723	0.959
32	Y	101	T	0.166	A	A	2.973	0.722	0.956
62	I	94	T	0.17	A	A	3.034	0.717	0.931
26	F	54	V	0.178	A	A	3.161	0.717	0.928
36	P	58	F	0.169	A	A	3.015	0.709	0.892
11	W	18	M	0.247	A	A	4.308	0.709	0.89
67	A	83	V	0.166	A	A	2.976	0.707	0.879
57	Q	104	M	0.175	A	A	3.109	0.703	0.861
50	P	63	V	0.16	A	A	2.873	0.701	0.852
62	I	98	S	0.157	A	A	2.823	0.69	0.801
42	F	109	I	0.181	A	A	3.211	0.689	0.794
68	T	94	T	0.158	A	A	2.843	0.686	0.784
43	V	50	P	0.151	A	A	2.727	0.685	0.775
11	W	17	L	0.239	A	A	4.169	0.681	0.759
44	K	57	Q	0.159	A	A	2.849	0.68	0.754
68	T	91	K	0.153	A	A	2.75	0.679	0.751

Table S2. Primers used for this study.

Site Directed Mutagenesis of ETR1	
Name	**Sequence (5'-3')**
D25N-Forward	ATACATCTCCAATTTCTTCATTGCG
D25N-Reverse	TGGTATTTCATTAACAATTCATCC
D25Q-Forward	ATACATCTCCAATTTCTTCATTGCGATTG
D25Q-Reverse	TGGTATTTCATTAACAATTCATCC
D25E-Forward	ACATCTCCGAATTCTTCATTGC
D25E-Reverse	ATTGGTATTTCATTAACAATTCATC
D25A-Forward	ATACATCTCCGCTTTCTTCATTGC
D25A-Reverse	ATTGGTATTTCATTAACAATTCATC
K91R-Forward	GACTACCGCGAGAGTGTTAACCGCTG
K91R-Reverse	TGGTATTTCATTAACAATTCATCC
K91M-Forward	GACTACCGCGATGGTGTTAACCG
K91M-Reverse	ATCACAAGCGCCACGGTT
K91A-Forward	GACTACCGCGGCTGTGTTAACCGCTG
K91A-Reverse	ATCACAAGCGCCACGGTT
Sequencing Primers for ETR1 mutagenesis	
ETR1-seq for pYCDE2	CCTTCCTTCATTCACGCACAC
ETR1-seq for pCAMBIA	CACCTTCGCGGTAGTCATCAC
Primers for analysis of CRISPR-Cas9 lines	
ERS1-Forward	CCTTCCTTCATTCACGCACAC
ERS1-Reverse	CACCTTCGCGGTAGTCATCAC
ERS2-Forward	CACCTTCGCGGTAGTCATCAC
ERS2-Reverse	CCTTCCTTCATTCACGCACAC
KanR-Forward	CACCTTCGCGGTAGTCATCAC
KanR-Reverse	CACCTTCGCGGTAGTCATCAC
Quantitative real time PCR	
β-tubulin-Forward	TGGTGGAGCCTTACAACGCTACTT
β-tubulin-Reverse	TTCACAGCAAGCTTACGGAGGTCA
ERF1-Forward	TCTAATCGAGCAGTCCACGCAACA
ERF1-Reverse	AACGTCCCGAGCCAAACCCTAATA
ARGOS-Forward	GTCATGGACGTCGGAAGAAACAAC
ARGOS-Reverse	GGGAACCAATAGCAGCATAAACGG
OSR1-Forward	ATGAGGGTTCATGATCAACGGCTG
OSR1-Reverse	GGCTGGGCTCATTAGAAGGAGAAA
EXP5-Forward	CACTCATACTTTAACTTGGTGTTGG
EXP5-Reverse	GACCATTGAGATAAGAGTTGCTTTG
EXPb1-Forward	GCAAATACAGAGGGAAGAACATA
ExPb1-Reverse	CTTCATCGATATCCACTCCTTAGA
CAPE2-Forward	TGACCACGACTCCTTGCAGTTCTT
CAPE2-Reverse	ATGAAGATCCCACCATTGTCGCAC
ERS1-Forward	TTCAGTCTACAAGCGATCTTTGAAGAGG
ERS1-Reverse	AGCGCGACAAACCGTTTACAGAGA
ERS2-Forward	ACACATTCTGGGAAACAGTAATCG
ERS2-Reverse	AAGCTACCGTCGTCTTCTGC

Movie S1 (separate file). AlphaFold-Multimer-based model of the ETR1 homodimer (coppers interacting).

Movie S2 (separate file). AlphaFold-Multimer-based model of the ETR1 homodimer (coppers not interacting).

SI References

1. A. B. Bleecker, M. A. Estelle, C. Somerville, H. Kende, Insensitivity to ethylene conferred by a dominant mutation in *Arabidopsis thaliana*. *Science* **241**, 1086-1089 (1988).
2. C. Chang, S. F. Kwok, A. B. Bleecker, E. M. Meyerowitz, Arabidopsis ethylene response gene *ETR1*: Similarity of product to two-component regulators. *Science* **262**, 539-544 (1993).
3. J. Hua, E. M. Meyerowitz, Ethylene responses are negatively regulated by a receptor gene family in *Arabidopsis thaliana*. *Cell* **94**, 261-271 (1998).
4. B. P. Hall *et al.*, Histidine kinase activity of the ethylene receptor ETR1 facilitates the ethylene response in Arabidopsis. *Plant Physiol* **159**, 682-695 (2012).
5. G. E. Schaller, B. M. Binder, Inhibitors of Ethylene Biosynthesis and Signaling. *Methods Mol Biol* **1573**, 223-235 (2017).
6. B. M. Binder, L. A. Mortimore, A. N. Stepanova, J. R. Ecker, A. B. Bleecker, Short-term growth responses to ethylene in Arabidopsis seedlings are EIN3/EIL1 independent. *Plant Physiol* **136**, 2921-2927 (2004).
7. B. M. Binder *et al.*, Arabidopsis seedling growth response and recovery to ethylene. A kinetic analysis. *Plant Physiol* **136**, 2913-2920 (2004).
8. X. Qu, G. E. Schaller, Requirement of the histidine kinase domain for signal transduction by the ethylene receptor ETR1. *Plant Physiol* **136**, 2961-2970 (2004).
9. S. J. Clough, A. F. Bent, Floral dip: a simplified method for Agrobacterium-mediated transformation of Arabidopsis thaliana. *Plant J* **16**, 735-743 (1998).
10. G. E. Schaller, A. B. Bleecker, Ethylene-binding sites generated in yeast expressing the Arabidopsis *ETR1* gene. *Science* **270**, 1809-1811 (1995).
11. F. Winston, C. Dollard, S. L. Ricupero-Hovasse, Construction of a set of convenient Saccharomyces cerevisiae strains that are isogenic to S288C. *Yeast* **11**, 53-55 (1995).
12. H. Liu *et al.*, CRISPR-P 2.0: An Improved CRISPR-Cas9 Tool for Genome Editing in Plants. *Mol Plant* **10**, 530-532 (2017).
13. C. J. Denbow *et al.*, Gateway-Compatible CRISPR-Cas9 Vectors and a Rapid Detection by High-Resolution Melting Curve Analysis. *Front Plant Sci* **8**, 1171 (2017).
14. C. LeBlanc *et al.*, Increased efficiency of targeted mutagenesis by CRISPR/Cas9 in plants using heat stress. *Plant J* **93**, 377-386 (2018).
15. I. Kasajima, Y. Ide, N. Ohkama-Ohtsu, T. Yoneyama, T. Fujiwara, A protocol for rapid DNA extraction from *Arabidopsis thaliana* for PCR analysis. *Plant Mol Biol Rep* **22**, 49-52 (2004).
16. R. L. Gamble, M. L. Coonfield, G. E. Schaller, Histidine kinase activity of the ETR1 ethylene receptor from Arabidopsis. *Proc. Natl. Acad. Sci. USA* **95**, 7825-7829 (1998).
17. S. N. Shakeel *et al.*, Ethylene Regulates Levels of Ethylene Receptor/CTR1 Signaling Complexes in Arabidopsis thaliana. *J Biol Chem* **290**, 12415-12424 (2015).
18. Y. F. Chen, M. D. Randlett, J. L. Findell, G. E. Schaller, Localization of the ethylene receptor ETR1 to the endoplasmic reticulum of Arabidopsis. *J Biol Chem* **277**, 19861-19866 (2002).
19. S. Schott-Verdugo, L. Muller, E. Classen, H. Gohlke, G. Groth, Structural Model of the ETR1 Ethylene Receptor Transmembrane Sensor Domain. *Scientific reports* **9**, 8869 (2019).
20. B. M. Binder, G. E. Schaller, Analysis of Ethylene Receptors: Ethylene-Binding Assays. *Methods Mol Biol* **1573**, 75-86 (2017).
21. C. Hadfield, A. M. Cashmore, P. A. Meacock, An efficient chloramphenicol-resistance marker for *Saccharomyces cerevisiae* and *Escherichia coli*. *Gene* **45**, 149-158 (1986).

22. M. I. Rai *et al.*, The ARGOS gene family functions in a negative feedback loop to desensitize plants to ethylene. *BMC Plant Biol* **15**, 157 (2015).
23. T. A. Hopf *et al.*, The EVcouplings Python framework for coevolutionary sequence analysis. *Bioinformatics* **35**, 1582-1584 (2019).
24. S. Ovchinnikov, H. Kamisetty, D. Baker, Robust and accurate prediction of residue-residue interactions across protein interfaces using evolutionary information. *eLife* **3**, e02030 (2014).
25. R. Evans *et al.*, Protein complex prediction with AlphaFold-Multimer. *bioRxiv* https://doi.org/10.1101/2021.10.04.463034, 2021.2010.2004.463034 (2021).
26. J. Jumper *et al.*, Highly accurate protein structure prediction with AlphaFold. *Nature* **596**, 583-589 (2021).
27. E. F. Pettersen *et al.*, UCSF ChimeraX: Structure visualization for researchers, educators, and developers. *Protein Sci* **30**, 70-82 (2021).